RAPID COMMUNICATIONS IN MASS SPECTROMETRY
*Rapid Commun. Mass Spectrom.* 2003; **17**: 1411–1415
Published online in Wiley InterScience (www.interscience.wiley.com). DOI: 10.1002/rcm.1063

# Magic bimetallic cluster anions of M/Pb (M = Au, Ag and Cu) observed and analyzed by laser ablation and time-of-flight mass spectrometry

**Xiaopeng Xing†, Zhixin Tian†, Hongtao Liu† and Zichao Tang***

State Key Laboratory of Molecular Reaction Dynamics, Center of Molecular Science, Institute of Chemistry, Chinese Academy of Sciences, Beijing 100080, People's Republic of China

Received 26 February 2003; Revised 17 April 2003; Accepted 17 April 2003

**By using laser ablation on mixtures of coinage metals M (Cu, Ag, Au) and lead, M/Pb binary cluster anions containing up to tens of atoms were produced and analyzed. Most of the magic clusters discovered can be described based on the electron shell models which were deduced from simple homogeneous metal cluster systems. The clustering activities of coinage metals and lead were also compared with the properties of their bulk binary alloys. Copyright © 2003 John Wiley & Sons, Ltd.**

Recently, intense research efforts have indicated that nanoclusters are attractive building blocks for self-assembled materials. Magic clusters that interact weakly can serve as suitable building blocks,[1,2] so one of the biggest challenges is to discover and synthesize clusters of this kind. Nanoclusters of coinage metals, especially gold,[3–5] are involved widely in these studies. Usually, the properties of coinage metal clusters can be described using electron shell models,[6,7] and the clusters with closed electron shells (total valence electron numbers are 1p, 8; 1d, 18; 2s, 20; 1f, 34; 2p, 40; 1g, 58; 2d, 68, etc., in the shell model for spherical clusters and 8, 14, 18, 20, 26, 30, 34, 36, 38, 40, 50, 54, 58, etc., in the ellipsoidal Clemenger-Nilsson shell model) have higher stability, i.e., appear as magic clusters in mass spectra.

Very recently, Lai-Sheng Wang *et al*.[8] showed that a 20-atom gold cluster produced by laser ablation was highly stable and chemically inert, and could even be comparable with $C_{60}$. Also, $W{\cdot}Au_{12}$ clusters were found to be another candidate that could be used to synthesize a cluster-assembled material.[9,10] Both $Au_{20}$ and $W{\cdot}Au_{12}$ have closed electron shells and have highly symmetrical structures. Lead is undoubtedly another important metal in this context, and its clusters have also attracted great attention.[11–16] The stability of magic cluster species of lead (containing 7, 13 and 19 atoms) has been explained assuming the closed polyhedron structures.[12,13] In our earlier studies,[17,18] similar structures were also used to explain the magic cluster species in M/Pb binary clusters containing one or two transition metals M (M = Co, Ti, Cr, Mn, Fe, Co, Ni, Cu, Zn, Pd, Ag, etc.). However, the magic cluster species present in the $Pb_n^{2+}$ system (n = 9, 15, 23, 27, 35) satisfy exactly the closed electron shells criterion.[16]

In this study, production and analysis of Au/Pb binary cluster anions (containing tens of atoms) were achieved using a home-made apparatus including a laser vaporization ion source and a high-resolution reflectron time-of-flight mass spectrometer (RTOFMS). In order to compare with Cu and Ag, M/Pb (M = Cu, Ag) binary cluster anions were also analyzed using this RTOFMS. Some new species other than those observed previously[18] were observed. The magic cluster species were investigated, and it was found that electron shell effects play an important role in these magic cluster species. The clustering activities of these metals were also compared with their corresponding bulk alloys.

## EXPERIMENTAL

The binary cluster anions of M/Pb (M = Cu, Ag, Au) were generated and analyzed under the following conditions. The samples were prepared with M (purity > 99.5%) and lead (purity > 99.8%) powders, mixed well in defined atomic ratios, and pressed into tablets. The experiments conducted to produce and detect Pb/M binary cluster anions were performed using a vaporization laser together with the home-made RTOFMS; a detailed description of this instrument has been given elsewhere.[19] Briefly, the second harmonic of a Q-switched Nd:YAG laser (532 nm, 10 mJ/pulse, 10 pulse/s) was focused on the surface of the tablet sample held in the vacuum chamber (at $10^{-6}$ Torr) of the spectrometer. The products were then extracted and accelerated to about 1.2 keV perpendicular to the cluster beam. Two sets of deflectors and einzel electrostatic lenses were used to guide and focus the ion beam. The ions were reflected by a reflector and a dual microchannel plate (MCP) detector was

**Correspondence to*: Z. Tang, State Key Laboratory of Molecular Reaction Dynamics, Center of Molecular Science, Institute of Chemistry, Chinese Academy of Sciences, Beijing 100080, People's Republic of China.
E-mail: zichao@mrdlab.icas.ac.cn
†Graduate student, Graduate Division, Chinese Academy of Sciences.

Contract/grant sponsor: National Natural Science Foundation of China; contract/grant number: 20203020.

RCM

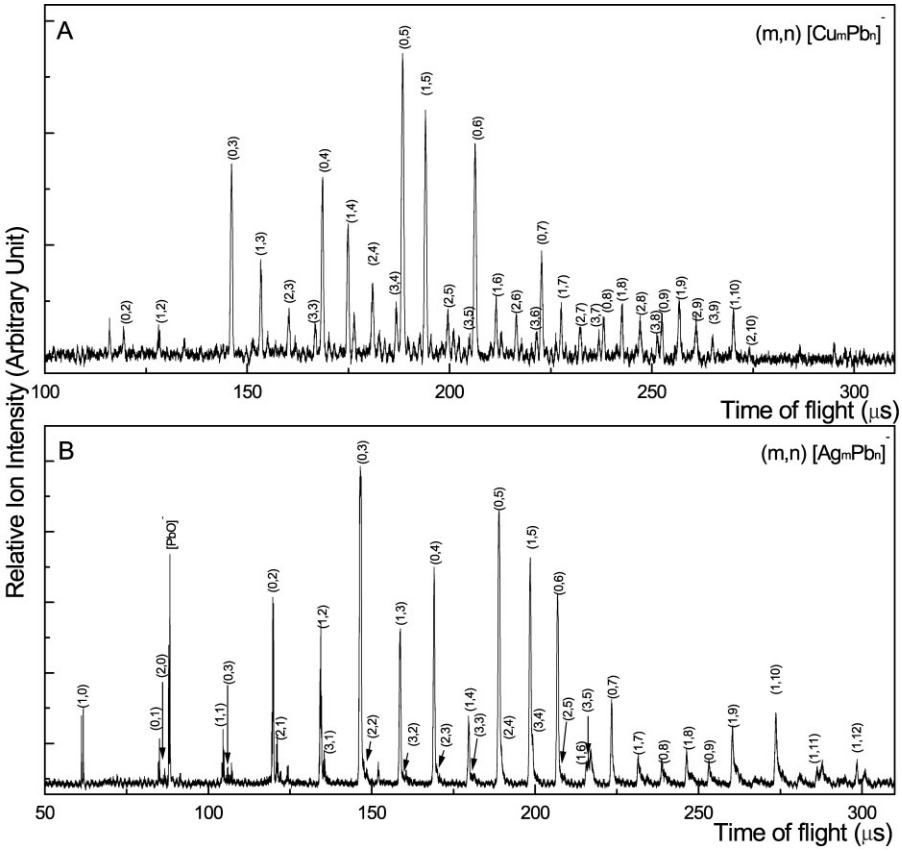


**Figure 1.** TOF mass spectra of binary cluster anions produced by laser ablation on mixed samples of (A) Cu/Pb (atomic ratio 1:1) and (B) Ag/Pb (atomic ratio 1:1).

installed at the space focus. Typically, the final digitized mass spectra were averaged over 300 laser pulses; the mass resolution of the spectrometer ($m/\Delta m$) is over 1000 under the present conditions. This enabled us to clearly resolve all products even in the high mass region.

## RESULTS AND DISCUSSION

Figures 1(A) and (B) show the mass spectra of the cluster anions resulting from the samples Cu/Pb and Ag/Pb, respectively. The atomic ratios of M/Pb (M = Cu or Ag) were 1:1. In both cases, the binary clusters containing 1, 2 and 3 coinage metal atoms were observed. Similarly to what was observed in our earlier work,[17,18] $Pb_n^-$ and $[MPb_n]^-$ were two dominant product series. However, the new species such as $[Cu_3Pb_n]^-$ and $[Ag_mPb_n]^-$ (m = 2, 3) can only be distinguished using this high-resolution mass spectrometer. It can be seen from Fig. 1 that the intensities of the binary cluster anions decrease with increasing numbers of the coinage metal atoms.

Figure 2 shows the mass spectrum of the cluster anions from the Au/Pb sample with atomic ratio 1:1. Clusters containing up to 25 atoms were detected. The low mass region ($m + n \leq 13$) and the high mass region ($m + n > 13$) of the spectrum are shown in Figs. 2(A) and 2(C), respectively. As a conspicuous difference from the binary cluster anions for the Cu/Pb or Ag/Pb systems, large abundances of gold-rich clusters were also observed. As an example, the mass spectral region corresponding to $m + n = 12$ is enlarged in Fig. 2(B); the possible compositions ($m = 1–12$, $n = 12–m$) are shown.

To make these trends more clear, the intensities of the cluster series $[MPb_n]^-$, $[M_2Pb_n]^-$ and $[M_3Pb_n]^-$ (M = Cu, Ag, Au), deduced from Figs. 1 and 2, are plotted in Fig. 3. It was found that the peak intensity distributions for the lead clusters with these three metals were very similar. Some apparent magic cluster species appear in each series. $[MPb_n]^-$ shows relatively intense peaks or sharp turning points at n = 5, 10 and 12; $[M_2Pb_n]^-$ and $[M_3Pb_n]^-$ show relatively intense peaks or sharp turning points at n = 1, 4 and 9. As for $[MPb_n]^-$, the magic cluster species present can be understood based on the geometrical structures of pure lead clusters. For example $Pb_5^{2-}$ can be regarded as a stable Zintl ion, and therefore the presence of less electronegative and single valence atoms M has the tendency to form $\{[Pb_5]^{2-}\ M^+\}$ cluster structures.[20] As for $[MPb_{10}]^-$ and $[MPb_{12}]^-$, based on the bi-capped square antiprism structure of $Pb_{10}$ and the icosahedron structure of $Pb_{13}$,[12,13] the lead packing cage structures with one transition metal inside was proposed.[17] However, the magic clusters observed in the $[M_2Pb_n]^-$ and $[M_3Pb_n]^-$ series are difficult to explain based only on this geometrical picture.[18]

The intensities of homogeneous gold clusters and the gold-rich binary clusters $[Au_m]^-$, $[Au_mPb]^-$ and $[Au_mPb_2]^-$, deduced from Fig. 2, are plotted in Fig. 4. The cluster distributions in these series display an odd-even alternation pattern over a large range (m = 3–21 for $[Au_m]^-$, m = 1–24 for $[Au_mPb]^-$, and m = 4–14 for $[Au_mPb_2]^-$). That is to say, the intensities of cluster anions containing odd numbers of gold atoms, which have even numbers of valence electrons, tend to be larger than those of neighboring clusters containing even

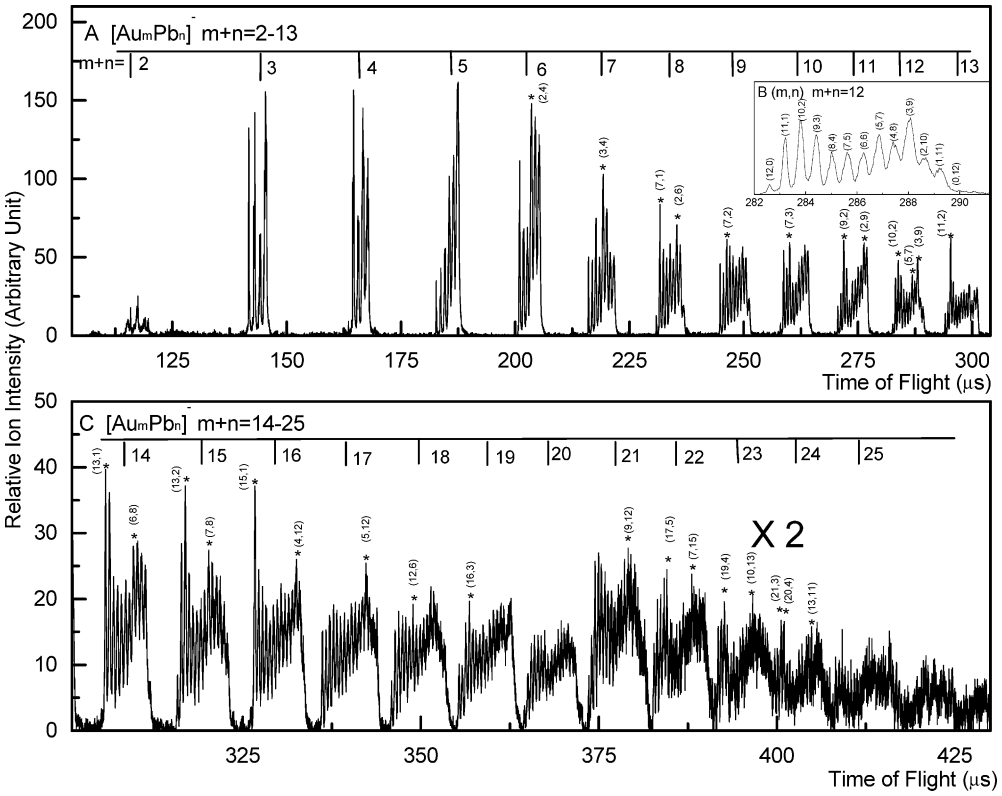


**Figure 2.** TOF mass spectra of binary cluster anions produced by laser ablation on a mixed sample of Au/Pb (atomic ratio 1:1): (A) total atom numbers $m+n \leq 13$, (B) $m+n=12$, and (C) $m+n>13$. Magic cluster peaks are labeled using *.

numbers of gold atoms and which thus have odd numbers of valence electrons. This effect demonstrates the electron-pairing effects on the stability of these clusters. Additionally, each of these three series has two higher intensity peaks that are followed at higher *m/z* by a steep decrease of ion intensities ($m=17$, 19 for $[Au_m]^-$, $m=13$, 15 for $[Au_mPb]^-$, and $m=9$, 11 for $[Au_mPb_2]^-$). The enhanced relative stability of $m=17$, 19 for pure coinage metal clusters was understood based on the electron shell model for spherical clusters, since they have 18 (1d closure) and 20 (2s closure) valence electrons,[6] respectively. However, it is very interesting that, if the s and p electrons of the lead atoms are included in the electron shells, $[Au_mPb]^-$ ($m=13$, 15) and $[Au_mPb_2]^-$ ($m=9$, 11) also have 18 and 20 valence electrons. The other peaks with possible closed electron shells ($Au_7^-$ and $[Au_3Pb]^-$, 1p(8) closure) were also found to be local maximum peaks in the mass spectra (labeled in Fig. 4).

Now we consider the unexplained magic cluster peaks in the cases of $[M_2Pb_n]^-$ and $[M_3Pb_n]^-$ (M = Cu, Ag and Au) in Fig. 3. $[M_3Pb_n]^-$ anions ($n=1$, 4 and 9) have totals of valence electrons of 8, 20 and 40, respectively, which also correspond to 1p, 2s and 2p closure. $[M_2Pb_n]^-$ clusters ($n=1$, 4 and 9) have totals of valence electrons of 7, 19 and 39, respectively. These are the nearest compositions to the electron shell closure criterion possible in this series because, with one more lead atom (with 4 valence electrons) added, building another new shell will thus begin conferring lower stability on the cluster system.[6]

In addition to the series mentioned above, all Au/Pb binary cluster groups containing equal total numbers of atoms were also studied. The cluster intensities in these groups do not change continuously with increasing numbers of one kind of constituent atom, and many magic cluster peaks are observed. It should be pointed out that the total electron numbers can only change by steps of 3 in each group, because when one gold atom is substituted by one lead atom the total electron numbers will increase by 3. Most of the magic clusters are labeled using an asterisk in Figs. 2(A) and 2(B). Their total valence electron numbers, and comparisons with the stable points proposed based on electron shell models, are summarized in Table 1. It is shown that, with the exception of $[Au_2Pb_6]^-$, $[Au_{13}Pb_2]^-$ and $[Au_{10}Pb_{13}]^-$, the total valence electron numbers for these magic clusters are exactly those corresponding to closed electron shells or just one or two fewer. This implies that the spherical shell model and ellipsoidal Clemenger-Nilsson shell model,[6] which were deduced from the simple homogeneous metal cluster systems, can also explain the stability of M/Pb (M = Cu, Ag and Au) binary magic clusters.

Even though they are only semiclassical approaches, these electron shell models usually allow for a more transparent interpretation of many phenomena and offer better insights into the important physical mechanisms than the purely microscopic theories. Our results show that they can explain well the relative stabilities of M/Pb (M = Cu, Ag and Au) anion clusters. Accordingly, some properties of these binary clusters can be deduced. First, they should be three-dimensional structures without major deviations from spherical shape. Second, all the valence electrons are strongly delocalized over the whole cluster; that is to say, the M/Pb (M = Cu, Ag and Au) binary cluster anions are to be regarded as one integrated species, both geometrically and electronically.

RCM

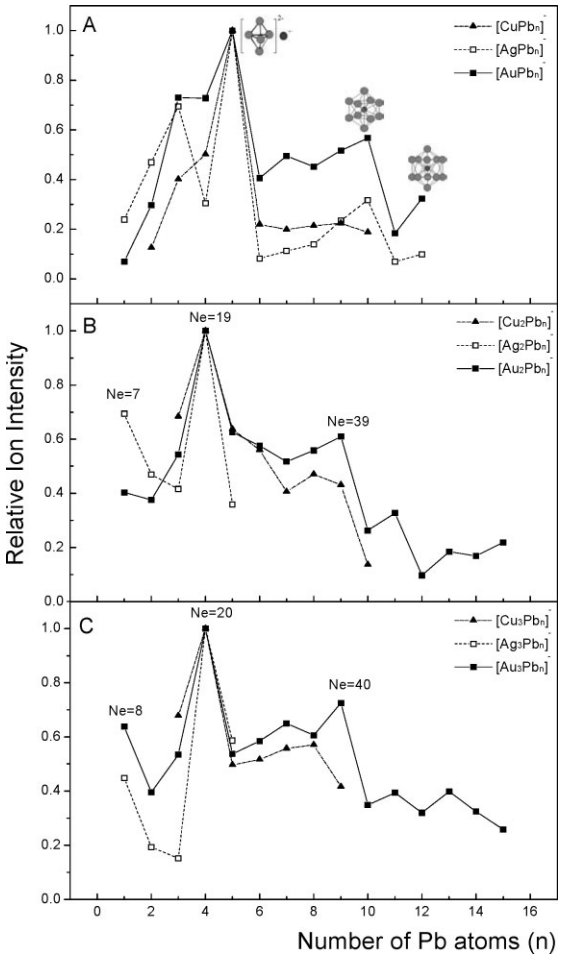


**Figure 3.** Relative intensities of (A) $[MPb_n]^-$, (B) $[M_2Pb_n]^-$, and (C) $[M_3Pb_n]^-$ series (M = Au, Ag, Cu) deduced from the experimental results. The absolute intensity of the highest peak in each series was defined as 1. The proposed structures of the magic cluster peaks in $[MPb_n]^-$ and the total valence electron numbers (Ne) of the magic cluster peaks in $[M_2Pb_n]^-$ and $[M_3Pb_n]^-$ are also listed.

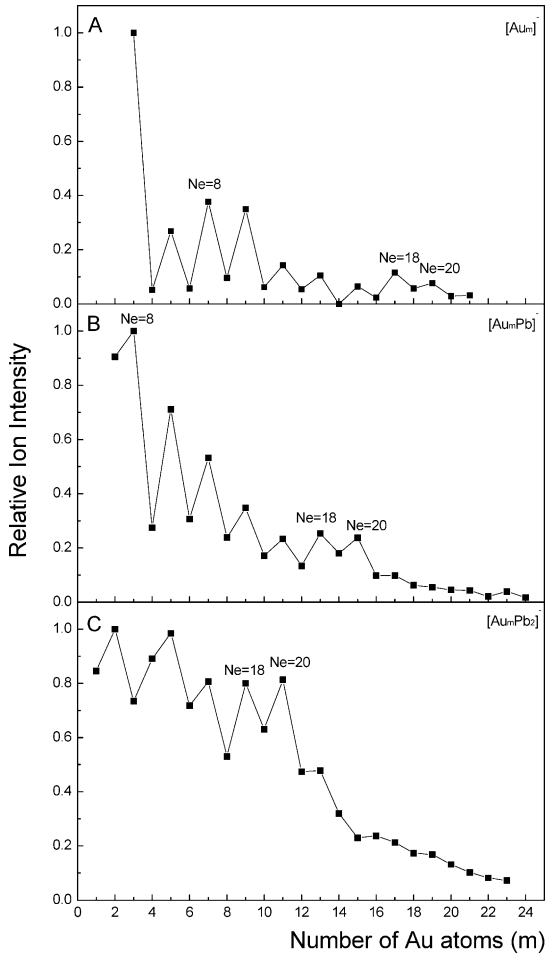


**Figure 4.** Relative intensities of (A) $[Au_m]^-$, (B) $[Au_mPb]^-$, and (C) $[Au_mPb_2]^-$ series deduced from the experimental results. The absolute intensity of the highest peak in each series was defined as 1. The total valence electron numbers (Ne) of the magic cluster peaks are also listed.

Another interesting phenomenon observed for the Au/Pb clusters was that, in the groups containing more than eight total atoms ($m + n \geq 8$), the peak intensities show a U-shaped distribution, as shown in Fig. 2. The ion intensity maxima appear in the gold-rich and lead-rich regions, while the ion intensity minimum appears where the numbers of atoms of gold and lead are nearly equal. In the present experiments, Pb/Au samples (1:1 atomic ratio in the case of Fig. 2) were vaporized into the gas phase where the atomic or ionic particles collide and combine with one another; therefore, on purely statistical grounds, the distribution of $[Au_mPb_n]^-$ clusters should appear as an *inverted* U-shape, and the formation of those clusters containing nearly equal numbers of lead and gold atoms should be favored. Our results show the opposite, and thus that self-combination processes of Au or Pb are more favorable than the inter-element combination processes between Au and Pb species. This is possibly due to thermodynamic rather than kinetic (statistical) reasons.

The distributions of these bimetallic clusters can also be compared with the corresponding bulk alloys. From our results, it can be seen that the clustering activities of Au/Pb are conspicuously different from those of the Ag/Pb or Cu/Pb systems. Au and Pb atoms can mix efficiently since all possible compositions were observed in the mass spectra, while laser ablation of Ag/Pb or Cu/Pb can only produce clusters containing fewer than three coinage metal atoms. In the bulk solid, copper or silver can only form alloys which contain less than 10% weight percent lead,[21] while gold and lead can form several kinds of alloys represented by formulae such as $Au_2Pb$, $AuPb_2$ and $AuPb_3$, etc.[22] These observations imply that Au/Pb can mix more efficiently than Cu/Pb or Ag/Pb, no matter whether in nanoclusters or in the bulk alloys. On the other hand, the compositions of the cluster anions are conspicuously different from those of the solid alloys. For example, Cu/Pb or Ag/Pb tend to form coinage metal-rich bulk alloys but form lead-rich clusters; Pb/Au can form clusters with arbitrary composition but can only form bulk alloys with certain specific formulae. This illustrates typical differences between the nano-scale metal particles and the macro-scale metal alloys.

**Table 1.** Total valence electron numbers in the magic clusters and comparison with stable points (total valence electron numbers) in the shell model for spherical clusters and the ellipsoidal Clemenger-Nilsson shell model. In column 3, the number in brackets is the stable point (total valence electron numbers) in the shell model for spherical clusters. In column 4, the number in bracket is the stable point (total valence electron numbers) in the ellipsoidal Clemenger-Nilsson shell model

| Compositions of magic clusters (m,n): $[Au_mPb_n]^-$ | Total valence electrons | Stable points in spherical cluster model | Stable points in Clemenger-Nilsson shell model |
|---|---|---|---|
| (2,4) | 19 | 2s(20)-1 | (20)-1 |
| (3,4) | 20 | 2s(20) | (20)-1 |
| (7,1) | 12 | | (14)-2 |
| (2,6) | 27 | — | — |
| (7,2) | 16 | 1d(18)-2 | (18)-2 |
| (7,3) | 20 | 2s(20) | (20) |
| (9,2) | 18 | 1d(18) | (18) |
| (2,9) | 39 | 2p(40)-1 | (40)-1 |
| (10,2) | 19 | 2s(20)-1 | (20)-1 |
| (5,7) | 34 | 1f(34) | (34) |
| (3,9) | 40 | 2p(40) | (40) |
| (11,2) | 20 | 2s(20) | (20) |
| (13,1) | 18 | 1d(18) | (18) |
| (6,8) | 39 | 2p(40)-1 | (40)-1 |
| (13,2) | 22 | — | — |
| (7,8) | 40 | 2p(40) | (40) |
| (15,1) | 20 | 2s(20) | (20) |
| (4,12) | 53 | | (54)-1 |
| (5,12) | 54 | | (54) |
| (12,6) | 37 | | (38)-1 |
| (16,3) | 29 | | (30)-1 |
| (9,12) | 58 | 1g(58) | (58) |
| (17,5) | 38 | | (38) |
| (7,15) | 68 | 2d(68) | (68) |
| (19,4) | 36 | | (36) |
| (10,13) | 63 | | — |
| (21,3) | 34 | 1f(34) | (34) |
| (20,4) | 37 | | (38)-1 |
| (13,11) | 58 | 1g(58) | (58) |

## CONCLUSIONS

M/Pb (M = Cu, Ag and Au) binary cluster anions containing tens of metal atoms were produced and analyzed. Most of the magic cluster species in these bimetallic systems can be understood using the electron shell models which were deduced from the simple homogeneous metal cluster systems. The stability of these magic binary clusters presents the possibility to prepare useful bimetallic nanomaterials or devices. The distributions of these clusters were also compared with the compositions of their corresponding bulk alloys.

## Acknowledgements

The authors gratefully acknowledge the support of the National Natural Science Foundation of China under Grant 20203020. We are indebted to Professor Qihe Zhu and Zhen Gao for their original design and assembly of the experimental apparatus. We are also indebted to Professor Hongfei Wang and Fanao Kong for their helpful discussions.

## REFERENCES

1. Sattler K. *Cluster Assembled Materials*, Trans Tech Publications: Enfield, New Hampshire, 1996.
2. Khanna SN, Jena P. *Phys. Rev. Lett*. 1992; **69**: 1664.
3. Chen S, Ingram RS, Hostetler MJ, Pietron JJ, Murray RW, Schaaff TG, Khoury JT, Alvarez MM, Whetten RL. *Science* 1998; **280**: 2098.
4. Garzon IL, Michaelian K, Beltrán MR, Posada-Amarillas A, Ordejón P, Artacho E, Sánchez-Portal D, Soler JM. *Phys. Rev. Lett*. 1998; **81**: 1600.
5. Gardea-Torresdey JL, Parsons JG, Gomez E, Peralta-Videa I, Troiani HE, Santiago P, Jose MY. *Nano Letters* 2002; **2**: 397.
6. De Heer WA. *Rev. Mod. Phys*. 1993; **65**: 611.
7. Taylor KJ, Pettiette-Hall CL, Cheshnovsky O, Smalley RE. *J. Chem. Phys*. 1992; **96**: 3319.
8. Li J, Li X, Zhai HJ, Wang LS. *Science* 2003; **299**: 864.
9. Pyykkö P, Runeberg N. *Angew. Chem. Int. Ed. Engl*. 2002; **41**: 2174.
10. Li X, Kiran B, Li J, Zhai HJ, Wang LS. *Angew. Chem. Int. Ed. Engl*. 2002; **41**: 4786.
11. Ganteför G, Gausa M, Meiwes-Broer KH, Lutz HO. *Z. Phys. D* 1989; **12**: 405.
12. Phillips JC. *Chem. Rev*. 1986; **86**: 619.
13. Phillips JC. *J. Chem. Phys*. 1987; **87**: 1712.
14. Hing KL, Wheeler RG, Wilson WL, Duncan MA. *J. Chem. Phys*. 1987; **87**: 3401.
15. Farley RW, Ziemann P, Castleman AW, Jr. *Z. Phys. D* 1989; **14**: 353.
16. Rabin I, Schulze W, Winter B. *Phys. Rev. B* 1989; **40**: 10282.
17. Zhang X, Li GL, Xing XP, Zhao X, Tang ZC, Gao Z. *Rapid Commun. Mass Spectrom*. 2001; **15**: 2399.
18. Zhang X, Tang ZC, Gao Z. *Rapid Commun. Mass Spectrom*. 2003; **17**: 621.
19. Xing XP, Tian ZX, Liu P, Gao Z, Zhu QH, Tang ZC. *Chin. J. Chem. Phys*. 2002; **15**: 83.
20. Martin TP. *J. Chem. Phys*. 1985; **83**: 78.
21. Hayes FH, Lukas HL, Effenberg G, Petzow GZ. *Metallkunde* 1986; **77**: 749.
22. Legendre B, Souleau C. *Bull Soc. Chim. Fr*. 1973; 2202.